10-13-2008

Nondestructive Evaluation of Aircraft Composites Using Transmissive Terahertz Time Domain Spectroscopy

Christopher D. Stoik *
Air Force Institute of Technology

Matthew J. Bohn
Air Force Institute of Technology

James L. Blackshire
Air Force Research Laboratory

Recommended Citation

Christopher D. Stoik, Matthew J. Bohn, and James L. Blackshire, "Nondestructive evaluation of aircraft composites using transmissive terahertz time domain spectroscopy," Opt. Express 16, 17039-17051 (2008).

Nondestructive evaluation of aircraft composites using transmissive terahertz time domain spectroscopy

Christopher D. Stoik[1*], Matthew J. Bohn[1] and James L. Blackshire[2]

[1]*Air Force Institute of Technology, Wright Patterson AFB, OH 45433, USA*
[2]*Air Force Research Laboratory, Materials and Manufacturing Directorate, Wright Patterson AFB, OH 45433, USA*
[*]*Corresponding Author: christopher.stoik@afit.edu*

Abstract: Terahertz time domain spectroscopy (TDS) was assessed as a nondestructive evaluation technique for aircraft composites. Damage to glass fiber was studied including voids, delaminations, mechanical damage, and heat damage. Measurement of the material properties on samples with localized heat damage showed that burning did not change the refractive index or absorption coefficient noticeably; however, material blistering was detected. Voids were located by TDS transmissive imaging using amplitude and phase techniques. The depth of delaminations was measured via the timing of Fabry-Perot reflections after the main pulse. Evidence of bending stress damage and simulated hidden cracks was also detected with terahertz imaging.

OCIS codes: (110.6795) Terahertz imaging; (120.4290) Nondestructive testing; (300.6495) Spectroscopy, terahertz.

References and links

1. W. Chan, J. Deibel, D. Mittleman, "Imaging with terahertz radiation," Rep. Prog. Phys. **70**, 1325-1379 (2007).
2. S. Wietzke, C. Jordens, N. Krumbholz, B. Baudrit, M. Bastian, M. Koch, "Terahertz imaging: a new non-destructive technique for the quality control of plastic weld joints," J. Euro. Opt. Soc. **2**, 07013 (2007).
3. A. Cooney and J. Blackshire, "Advanced imaging of hidden damage under aircraft coatings," Proc. SPIE **617902**, 1-11 (2006).
4. F. Rutz, R. Koch, S. Khare, M. Moneke, H. Richter, U. Ewert, "Terahertz quality control of polymeric products," Int. J. Infrared Millim. Waves **27**, 547-556 (2006).
5. F. Rutz, T. Hasek, M. Koch, H. Richter, U. Ewert, "Terahertz birefringence of liquid crystal polymers," Appl. Phys. Lett. **89**, 221911 (2006).
6. A. Redo-Sanchez, N. Karpowicz, J. Xu, X. C. Zhang, "Damage and defect inspection with terahertz waves," presented at the Fourth International Workshop on Ultrasonic and Advanced Methods for Nondestructive Testing and Material Characterization, UMass Dartmouth, N. Dartmouth, MA, 19 June 2006.
7. D. Zimdars, J. White, G. Stuk, A. Chernovsky, G. Fichter, S. Williamson, "Large area terahertz imaging and non-destructive evaluation applications," presented at the Fourth International Workshop on Ultrasonic and Advanced Methods for Nondestructive Testing and Material Characterization, UMass Dartmouth, N. Dartmouth, MA, 19 June 2006.
8. M. Reiten, L. Hess, R. Cheville, "Nondestructive evaluation of ceramic materials using terahertz impulse ranging," Proc. SPIE **617905**, 1-8 (2006).
9. S. Wang and X. Zhang, "Pulsed terahertz tomography," J. Appl. Phys. D **37** R1-R36 (2004).
10. J. Pearce and D. Mittleman, "Propagation of single-cycle terahertz pulses in random media," Opt. Lett. **26**, 2002-2004 (2001).
11. J. Pearce and D. Mittleman, "Scale model experimentation: using terahertz pulses to study light scattering," Phys. Med. Biol. **47**, 3823-3830 (2002).
12. Y. C. Shen, P. F. Taday, M. Pepper, "Elimination of scattering effects in spectral measurement of granulated materials using terahertz time domain spectroscopy," Appl. Phys. Lett. **92**, 051103 (2008).
13. J. R. Fletcher, G. P. Swift, Dai De Chang, J. A. Levitt, J. M. Chamberlain "Propagation of terahertz radiation through random structures: an alternative theoretical approach and experimental validation," J. Appl. Phys. **101**, 013102 (2007).

#99960 - $15.00 USD Received 11 Aug 2008; revised 6 Oct 2008; accepted 6 Oct 2008; published 10 Oct 2008

14. K. J. Chau, S. Mujumdar, A. Y. Elezzabi, "Terahertz propagation in non-homogeneous strongly scattering media," Proc. SPIE **5727**, 177-185 (2005).
15. E. Tuncer, N. Bowler, I. J. Youngs, "Application of the spectral density function method to a composite system," Physica B **373**, 306-312 (2005).
16. R. Piesiewicz, C. Jansen, D. Mittleman, T. Kleine-Ostman, M. Koch, T. Kurner, "Scattering analysis for the modeling of thz communication systems," IEEE Trans. Ant. Prop. **55**, 3002-3009 (2007).
17. S. Lee, "Scattering by a dense layer of infinite cylinders at normal incidence," J. Opt. Soc. Am. A **25**, 1022-1029 (2008).
18. S. Wietzke, C. Jansen, F. Rutz, D. Mittleman, M. Koch, "Determination of additive content in polymeric compounds with terahertz time-domain spectroscopy," Polym. Test. **26**, 614-618 (2007).
19. V. Myroshnychenko and C. Brosseau, "Effective complex permittivity of two-phase random composite media: a test of the two exponent phenomenological percolation equation," J. Appl. Phys. **103**, 084112 (2008).
20. D. Aspnes, "The accurate determination of optical properties by ellipsometry," in *Handbook of Optical Constants of Solids*, E. Palik, ed. (Academic Press, Inc., Orlando, FL 1985).
21. D. Bruggeman, "Dielektrizitatskonstanten und Leitfahigkeiten der Mischkorper aus isotropen Substanzen," Ann. Phys. **24**, 636 (1935).
22. J. Baxter and C. Schmuttenmaer, "Conductivity of ZnO nanowires, nanoparticles, and thin films using time-resolved terahertz spectroscopy," J. Phys. Chem. B **110**, 25229-25239 (2006).
23. M. Kerker, *The Scattering of Light and other Electromagnetic Radiation* (Academic Press, Inc., San Diego, CA 1969).
24. M. Naftaly and R. Miles, "Terahertz time-domain spectroscopy of silicate glasses and the relationship to material properties," J. Appl. Phys. **102**, 043517 (2007).
25. D. Mittleman, "Terahertz imaging," in *Sensing with Terahertz Radiation*, D. Mittleman, ed. (Springer, New York, NY 2003).

1. Introduction

Composite materials such as fiberglass, Kevlar, and carbon fiber are increasingly being used as structural components in high performance military aircraft, because of their high strength to weight ratios, improved aerodynamic performance, increased safety, and reduced corrosion compared with other structural materials. However, composites can be weakened by various defects and stress during the lifecycle of an aircraft, and routine maintenance of composite materials requires rather complicated inspection and repair techniques. Terahertz (THz) radiation could have the unique ability to penetrate composites and identify defects such as voids, delaminations, mechanical damage, or heat damage [1-9]. THz offers a non-invasive, non-contact, non-ionizing method of assessing composite part condition and could overcome some of the short-comings of other non-destructive techniques such as x-rays, ultrasound, video inspection, eddy currents, and thermographic techniques.

A number of articles have been written which address the scattering of terahertz through random media and composites as well as efforts to model the dielectric properties of composites using effective medium theory [10-19]. Using a combination of effective medium theory and scattering theory, we explain the propagation of THz through a glass fiber composite. First, the material properties of weaved glass fiber, polyimide resin, and the glass fiber composite were measured separately using THz TDS. Next, effective medium approximations for the composite were used to show the correlation between the composite and its components. Finally, scattering theory calculations were made to show the minimal contribution of scattering to the extinction coefficient.

THz TDS has been investigated as a possible method of quality control of polymeric compounds and their composites by imaging [4,5]. THz, in both continuous wave and pulsed modes, has also been studied as a means of evaluating damage to carbon fiber composites [6]. We examined aircraft glass fiber composites with various forms of damage with our THz TDS system. The samples represent the outer shell of the panel of an aircraft, consisting mostly of the glass fiber composite with a thin outer coating. Refractive indices and absorption coefficients in the terahertz frequency range were measured using THz TDS in transmission configuration for comparison of damaged and undamaged material states. Results showed that localized heat damage did not change the material properties of the

#99960 - $15.00 USD Received 11 Aug 2008; revised 6 Oct 2008; accepted 6 Oct 2008; published 10 Oct 2008

composite sample noticeably, however, changes in the terahertz signal were observed due to material blistering, coating loss, and/or residue. A series of test samples were prepared, which included hidden voids/delaminations, and these defects could be located by TDS imaging using amplitude and phase analysis techniques. The depth of the delaminations could be measured via the timing of Fabry-Perot reflections after the main pulse. There was also evidence that areas of damage from bending stress and simulated hidden cracks (linear slit voids) could be detected with THz TDS imaging.

2. Theory and experiment

The THz TDS setup used to collect the material parameter data and perform the imaging is shown in Fig. 1. A Ti:Sapphire laser produced mode-locked, 100 femtosecond output pulses which were used to excite a photoconductive switch biased with 48 volts. The transmitted THz pulse was detected using an electro-optic technique (ZnTe crystal). A Fourier Transform could then be taken of the pulse to determine the amplitude spectrum of the THz pulse.

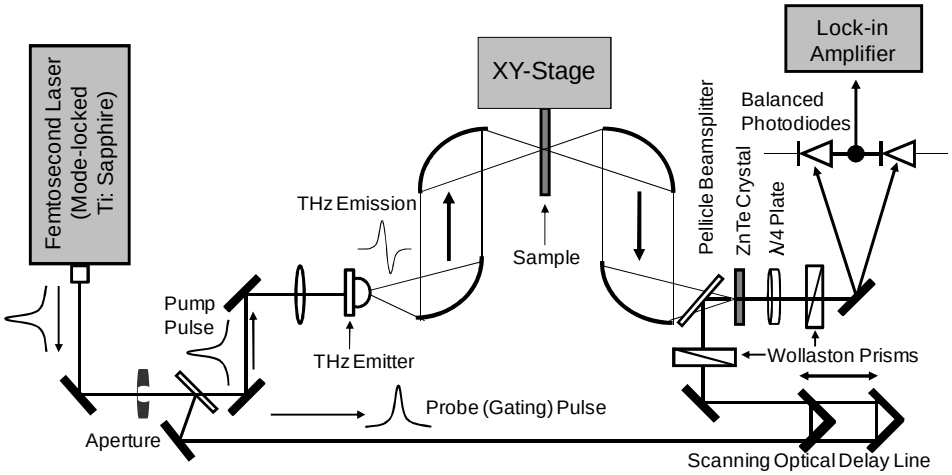

Fig. 1. THz TDS system used in transmission configuration for imaging and material parameter measurements.

By comparing the amplitude spectrum of a sample material to the reference signal with no sample, we could determine the material properties of the composite sample. The index of refraction $n(\omega)$ was calculated using the following equation

$$n(\omega) = 1 + \frac{c\left[\phi_{sam}(\omega) - \phi_{ref}(\omega)\right]}{\omega d} \tag{1}$$

where ϕ is the phase of the sample (*sam*) or the reference (*ref*), c is the speed of light, and d is the sample thickness. The absorption coefficient $\alpha(\omega)$ could then be calculated simultaneously with the index of refraction using the following formula

$$\alpha(\omega) = -\frac{2}{d}\ln\left[\frac{|E_{sam}(\omega)|}{T(\omega)|E_{ref}(\omega)|}\right] \tag{2}$$

in which $|E_{sam}(\omega)|$ is the magnitude of the THz field collected through the sample, $|E_{ref}(\omega)|$ is the magnitude of the THz field collected through air, and $T(\omega)$ is the fraction of the power transmitted through the air-sample interface. This transmitted fraction is given by

#99960 - $15.00 USD Received 11 Aug 2008; revised 6 Oct 2008; accepted 6 Oct 2008; published 10 Oct 2008

$$T(\omega) = \frac{4n(\omega)}{\left(n(\omega)+1\right)^2}. \tag{3}$$

Effective medium approximations are used to equate the dielectric properties of individual components to the dielectric properties of their composite material when the inclusions are small compared to the wavelength (< 0.1λ – 0.2λ) [20]. One of the approximations used, especially when the volume of inclusions is greater than 15%, is the Bruggeman model [21]. The equation for this model is

$$f\left(\frac{\varepsilon_i - \varepsilon_{eff}}{\varepsilon_i + K\varepsilon_{eff}}\right) + (1-f)\left(\frac{\varepsilon_h - \varepsilon_{eff}}{\varepsilon_h + K\varepsilon_{eff}}\right) = 0 \tag{4}$$

where f is the volume fraction of the inclusions, ε_i is the dielectric constant of the inclusion, ε_h is the dielectric constant for the host material, ε_{eff} is the effective medium approximation and K is the geometric factor. K is equal to 2 for a system with disorder and 1 if all of the cylinders are collinear with the incident radiation [22]. In our system, the glass fiber weave was considered as the inclusion and the polyimide was the host material. The glass fiber weave is made up of individual cylinders of glass that are approximately 10 μm in diameter and much smaller than the THz wavelength. These cylinders are then bundled together into groups that were about 600 μm in width which are then used to weave the overlapping pattern used in the composite. The polyimide resin is added and permeates throughout the individual glass fiber strands. The glass fiber volume concentration is typically between 40 – 60% depending on the type of technique used for combining the two components.

The effective medium approximation can be used to estimate the absorption coefficient and the index of refraction of the composite material; however, it would also be useful to determine the amount that scattering contributes to the extinction coefficient versus absorption. Since the diameters of the individual strands of glass (10 μm) are much smaller than the THz wavelengths used in this laboratory setup, it can be considered Rayleigh scattering. For infinitely long cylinders with sufficiently small diameters with respect to the wavelength, the scattering cross section per unit length σ can be estimated for the TE and TM modes:

$$\sigma_{TM} = \frac{2\pi^5 a^4}{\lambda^3}\left(m^2 - 1\right)^2 \tag{5}$$

$$\sigma_{TE} = \frac{4\pi^5 a^4}{\lambda^3}\left(\frac{m^2 - 1}{m^2 + 1}\right)^2 \tag{6}$$

where a is the radius of the cylinder, λ is the wavelength of the radiation, and m is the ratio of the index of refraction of the scattering center to the index of refraction of the containing medium [23]. The scattering coefficient μ_s can then be determined by

$$\mu_s(\omega) = \left[n_0 \sigma_s(\omega)\right] \tag{7}$$

in which n_0 is the density of inclusions and σ_s is the scattering cross section. An estimate of the scattering coefficient can be made if the host and inclusion dielectric constants and the inclusion density are known. The experimental measurement made in Eq. (2) determines the extinction coefficient μ_e, which is a combination of the scattering coefficient and the material absorption coefficient. It is related to the absorption coefficient by

#99960 - $15.00 USD Received 11 Aug 2008; revised 6 Oct 2008; accepted 6 Oct 2008; published 10 Oct 2008

$$\mu_e = \mu_s + \alpha \,. \tag{8}$$

In this experiment, since we were measuring composites, the scattering coefficient contribution was estimated in order to determine a more accurate absorption coefficient.

Polyimide is a resin which has the characteristic of being very resilient to thermal loads, maintaining its properties for long periods of continuous use at 230°C, and for short excursions as high as 480°C. One of the problems with designing aircraft is that the heat from jet engines can cause damage to the external structure of the aircraft. THz TDS could be used to measure the material properties of the aircraft glass fiber composites to determine if the composition of the material has fundamentally changed. Composite samples were prepared that were heated with various temperatures close to the maximum for polyimide for short durations. These samples are labeled 2 and 3 in Fig. 2. The first sample was burned at 440°C for 4 minutes, creating a blister on the sample about 2 cm X 1.5 cm. The second sample was burned in two places: 430°C for 6 minutes and 425°C for 20 minutes.

Another goal was to determine if various forms of damage could be imaged with a THz TDS system in transmission setup. Three additional samples were prepared to test the ability of a THz TDS system to detect the damage. The first composite specimen, labeled 1 in Fig. 2, was used as a thickness standard coupon to test the response of THz TDS imaging techniques to various sample thicknesses. Another coupon, labeled 5, was prepared to try to detect flaws. This coupon consisted of two laminated pieces. The bottom piece was prepared by etching four layers and then creating a 6 mm slit and a 3 mm flat bottom hole (~70 μm depth) in each of the four layers. A top layer was created by etching 4 layers with the same thicknesses and then attached to the bottom layer in the opposite direction with epoxy, being careful not to allow any epoxy into the flaws. Finally, a third sample, labeled 4 in Fig. 2, was

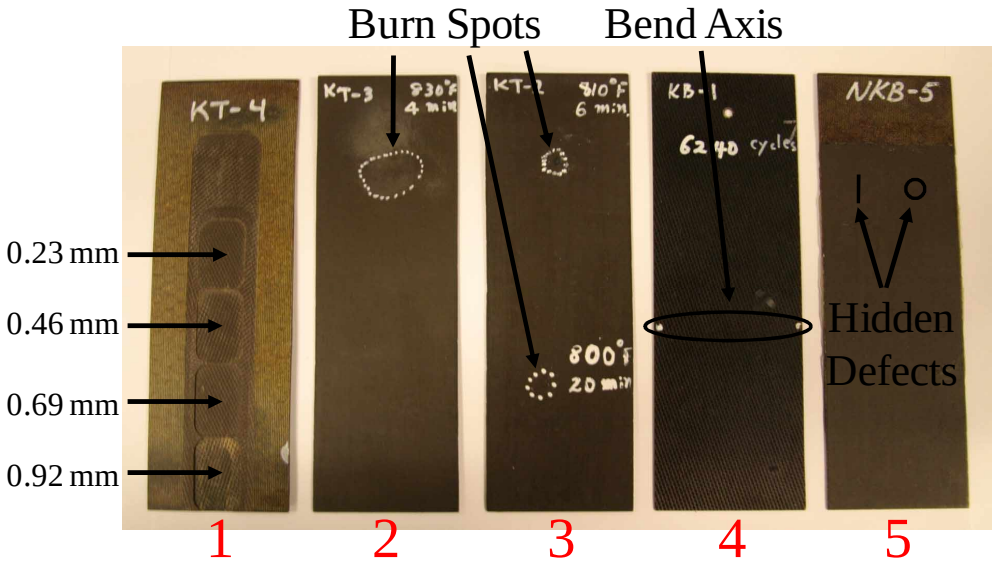

Fig. 2. Photograph showing the 5 glass fiber samples: (1) thickness calibration sample, (2) & (3) burn samples, (4) mechanical stress sample, and (5) hidden defect sample showing the hidden location of two of the eight defects.

prepared by bending a piece of glass fiber about a fixed axis a total of 6240 cycles to investigate bending damage with THz TDS imaging.

#99960 - $15.00 USD Received 11 Aug 2008; revised 6 Oct 2008; accepted 6 Oct 2008; published 10 Oct 2008

3. Results and discussion

3.1 Scattering approximations for glass fiber

In preparation for measuring material parameters, we first measured a THz pulse and its amplitude spectra for the air reference and compared it with the pulse and spectrum through undamaged glass fiber shown in Fig. 3. In an effort to determine the scattering effects of THz radiation in a glass fiber composite, samples of polyimide and glass fiber weave were prepared. The material parameters were determined first using THz TDS and thickness

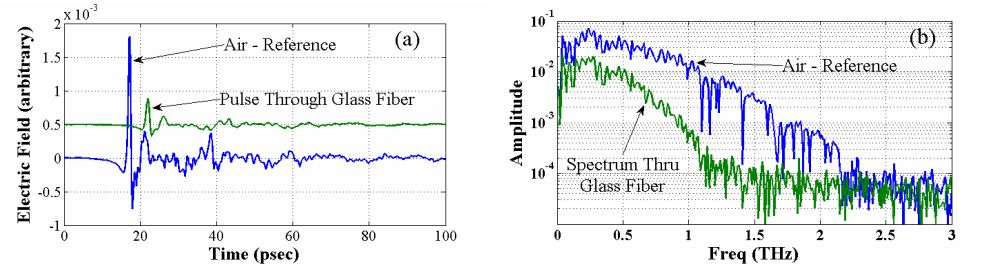

Fig. 3. THz TDS (a) pulse and (b) amplitude spectra for air reference and through glass fiber.

measurements. The results for polyimide (0.85 mm thick) in Fig. 4 show a refractive index that remained fairly constant between 1.79 – 1.82 and absorption coefficients of 3 cm^{-1} (0.5 THz), 7.5 cm^{-1} (0.8 THz), and 10.5 cm^{-1} (1.0 THz). It was difficult to obtain a thickness measurement on the weaved glass and therefore the refractive index and absorption coefficient in the THz region could not be accurately determined. Other measurements have been made on a variety of glasses [24], but no information is yet available on the glass used in this research. However, since the glass fiber composite could be measured, effective medium

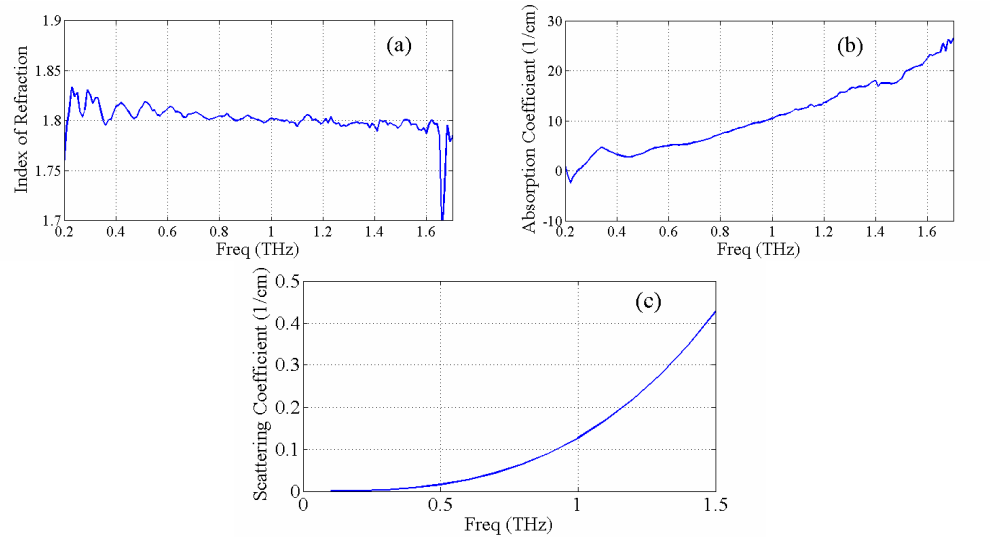

Fig. 4. THz TDS material parameter measurements using actual thickness measurements for polyimide showing (a) index of refraction and (b) absorption coefficient. The calculated scattering coefficient for the glass fiber composite is shown in part c.

theory was used to estimate the approximate dielectric properties of the glass. Then the glass and polyimide measurements were used to estimate the effects of scattering in the glass fiber

#99960 - $15.00 USD Received 11 Aug 2008; revised 6 Oct 2008; accepted 6 Oct 2008; published 10 Oct 2008

composite. Using the Bruggeman model with a glass fiber refractive index of 2.05, a polyimide index of 1.80, and assuming the composite is made up of 60% glass by volume (common for high performance composites), the refractive index for the glass was estimated to be 2.22. Using the values of the refractive index, the value of m, which appears in Eq. (5) and Eq. (6), was calculated to be 1.23. An estimate of the scattering coefficient for the glass fiber composite was then determined, assuming that the two perpendicular components of the scattering coefficient contributed equally, $\bar{\sigma} = (\sigma_{TM} + \sigma_{TE})/2$. This assumption was made based on the overlapping weave pattern of the glass. The results of the scattering approximation are shown in Fig. 4(c). Since the estimate was low in comparison to the extinction coefficient present in Fig. 4(b), scattering was considered to be insignificant in the glass fiber.

3.2 Burn diagnostics using material property measurements

After measuring the indices of refraction for the glass, polyimide, and composite, we investigated the burn samples to determine their material parameters. Thickness measurements were made on each of the samples and their burn areas, where the most visually noticeable difference was in the largest burn area (440°C for 4 minutes). Using the measured thickness of each blistered area, we obtained the results in Fig. 5 for the (a) index of refraction and (b) absorption coefficient. Figure 5 shows that there is a variation based on the thickness of the sample blister. The index of refraction for the unaltered composite remained relatively constant in the THz frequency range at 2.05 ± 0.01 while the absorption coefficient was measured as 17.5 ± 0.8 cm^{-1} (0.5 THz), 27.5 ± 1.1 cm^{-1} (0.8 THz) and 38 ± 1.6 cm^{-1} (1 THz). This is comparable to another measurement made on glass fiber samples, where the

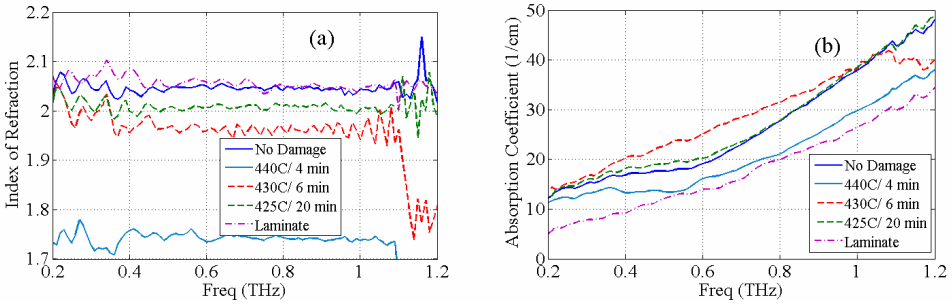

Fig. 5. THz TDS material parameter measurements using actual thickness measurements for burn damage areas showing (a) indices of refraction and (b) absorption coefficients.

index of refraction was 2.05-2.1 and the absorption coefficient was 12 cm^{-1} (0.5 THz) and 26-32 (0.8 THz) [4]. For comparison, the burned material parameter measurements were calculated with the undamaged sample thickness, such that the optical path length through each damage spot was constant. As is shown in Fig. 6, two of the burn areas have relatively the same optical path length as the undamaged area. The third damage area, burned at 430°C for 6 minutes, may have been different due to a small difference within the burn spot. There is an area in the center of the burn spot where there appears to be either a removal of the outer coating or a residue created during the burning process. Since it is in the center of the small burn spot it was not possible to ensure a THz TDS measurement could be made outside of the difference area. These measurements suggest that burning the samples at these high temperatures does not alter the material parameters, but merely introduces a blistering of the glass fiber and/or coating.

#99960 - $15.00 USD Received 11 Aug 2008; revised 6 Oct 2008; accepted 6 Oct 2008; published 10 Oct 2008

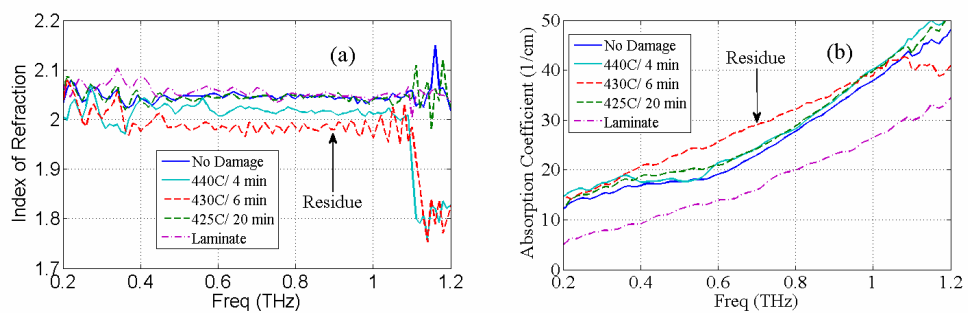

Fig. 6. THz TDS material parameter measurements, assuming the same thickness, for burn damage areas showing (a) indices of refraction and (b) absorption coefficients.

3.3 2-D transmissive imaging of defects

This subsection describes the THz imaging results from scanning the various defects outlined in section 2. This was accomplished using the THz TDS setup in Fig. 1 with a raster scanner to move the sample through the THz beam. The THz spot size was measured to be 1.5 mm and individual pixels were 1 X 1 mm in all of the scans except the calibration sample with 0.5 X 0.5 mm pixels. The first sample was prepared to calibrate the system based on material thickness. A THz image was taken of a 1 X 1 cm section of overlapping milled out areas with different thicknesses. The image is shown in Fig. 7 where (a) represents the peak pulse amplitude and (b) shows the pulse position at each pixel [25]. The decrease in amplitude of the pulse at the edges is a result of THz scattering [25]. Similar images can be shown using the area under the curve from the amplitude spectrum in the frequency domain. The differing heights of the edges of the milled out areas causes a frequency dependence in the amplitude intensity. The periodic modulation in Fig. 7(b) is a result of the interpolation technique to smooth out the pixels and does not match the pattern of the glass weave within the composite.

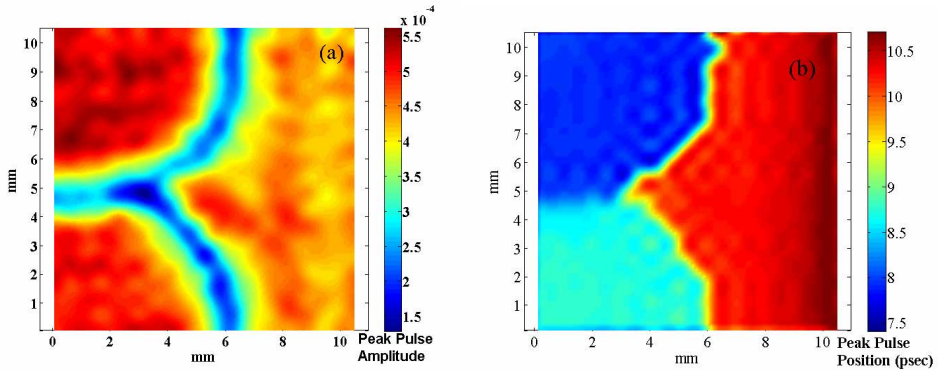

Fig. 7. THz TDS images showing a section of the glass fiber that had been milled to two different thicknesses using peak pulse amplitude (a) and peak pulse position (b) techniques.

The next task was to image the burn samples. The results of the burn dot images formed by the peak amplitude of the THz pulses are shown in Fig. 8 with the visibly burned areas within the circles. Figure 8(a) shows the sample that was burned at 440°F for 4 minutes over ~ 2 X 1.5 cm area. It has a visibly noticeable bubble or blister on its exterior which roughly corresponds with the blue area within the black oval. Comparisons of the THz time domain signal of pixels from the burn area were compared with those from outside the burn area. An example is shown in Fig. 9 contrasting a THz signal from an undamaged portion of the sample to one from the center of the large burn area (440°C for 4 minutes). There appeared to be time domain reflections within several of the pixels within the burn area, showing

#99960 - $15.00 USD Received 11 Aug 2008; revised 6 Oct 2008; accepted 6 Oct 2008; published 10 Oct 2008

evidence of air gaps, but without a consistent pattern between pixels. In the frequency domain, there were no consistent spectral changes to the THz signals through the burn areas. The other two burn areas are shown in Figs. 8(b) and 8(c), neither of which showed much visual evidence of blistering. The dark blue area within the circle in Fig. 8(b) is roughly equivalent to the position of the residue or coating loss. Since the absorption spectrum remained higher than the unburned sample, even when adjusted to the same optical path length, it is more likely that the dark blue area is a form of residue. The red circular dots in Fig. 8(c) and less noticeable orange dots in Fig. 8(b) correspond to the white marker dots made on the samples to show the extent of the burn area. The THz image of the damage area in Fig. 8(c) was inconclusive in showing evidence of burning.

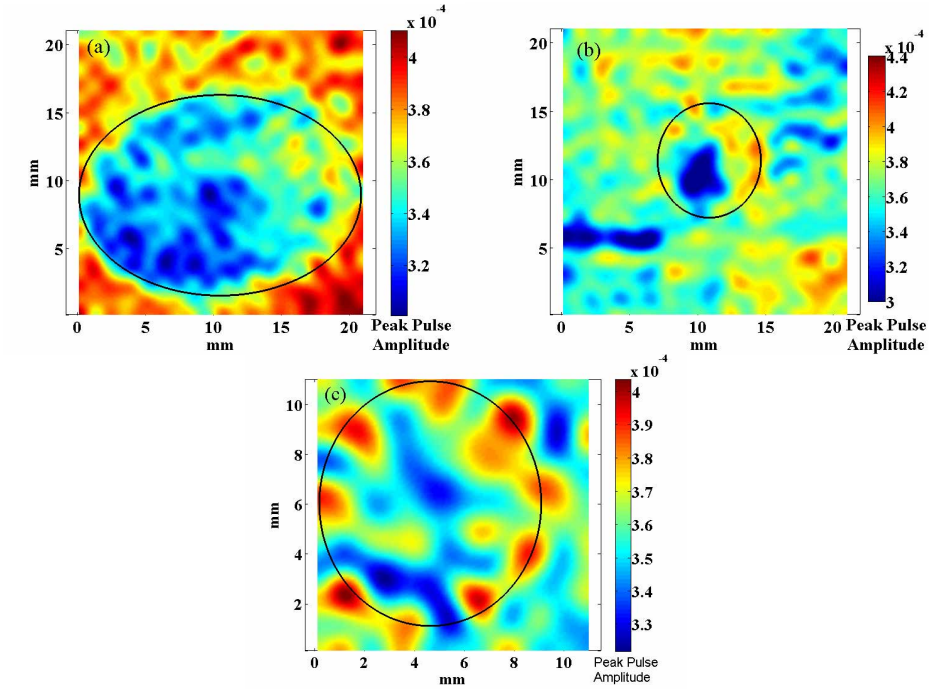

Fig. 8. THz TDS images for three burn areas on glass fiber samples: (a) 440°C for 4 minutes, (b) 430°C for 6 minutes, and (c) 425°C for 20 minutes.

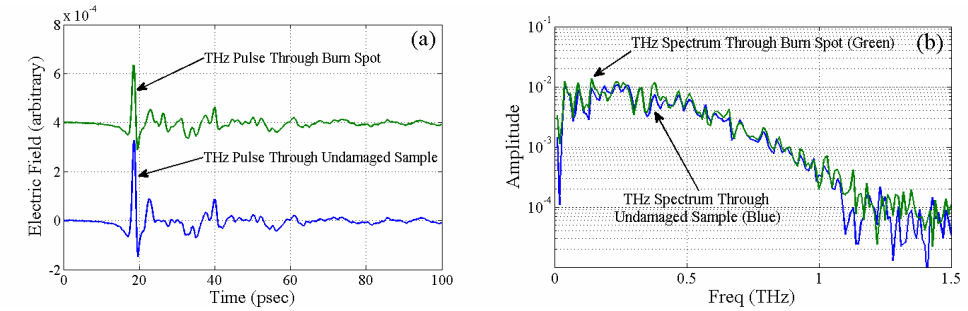

Fig. 9. THz TDS (a) pulse and (b) amplitude spectra for undamaged glass fiber sample and for an area with burn damage (440°C for 4 minutes).

Voids were also investigated, which simulate either manufacturing defects or damage caused by stress over time. THz images are shown in Figs. 10(a) and 10(b) for a circular void

#99960 - $15.00 USD Received 11 Aug 2008; revised 6 Oct 2008; accepted 6 Oct 2008; published 10 Oct 2008

(3 X 3 mm) and a (c) crack or slit void (6 mm length) in Fig. 10(c). For the circular void, a simple time domain amplitude or phase technique was sufficient to detect the void. For the slit void, a specific frequency range was required to isolate the approximate position, and was more difficult to isolate on multiple attempts [25]. The voids show an area of reduced amplitude, most likely due to the multiple reflections from the air/composite interface.

Finally, an attempt was made to show damage caused by mechanical fatigue as a result of 6240 bending cycles. Visually, one could observe a thin area of discoloration on one side of the glass fiber strip and one could see a small amount of cracking and buckling on the back side. In Fig. 11, the image of the sample shows an area of lesser amplitude corresponding roughly to where the axis of bending occurred. Electrical tape, in the shape of an 'X', was attached at the top of the image area for reference.

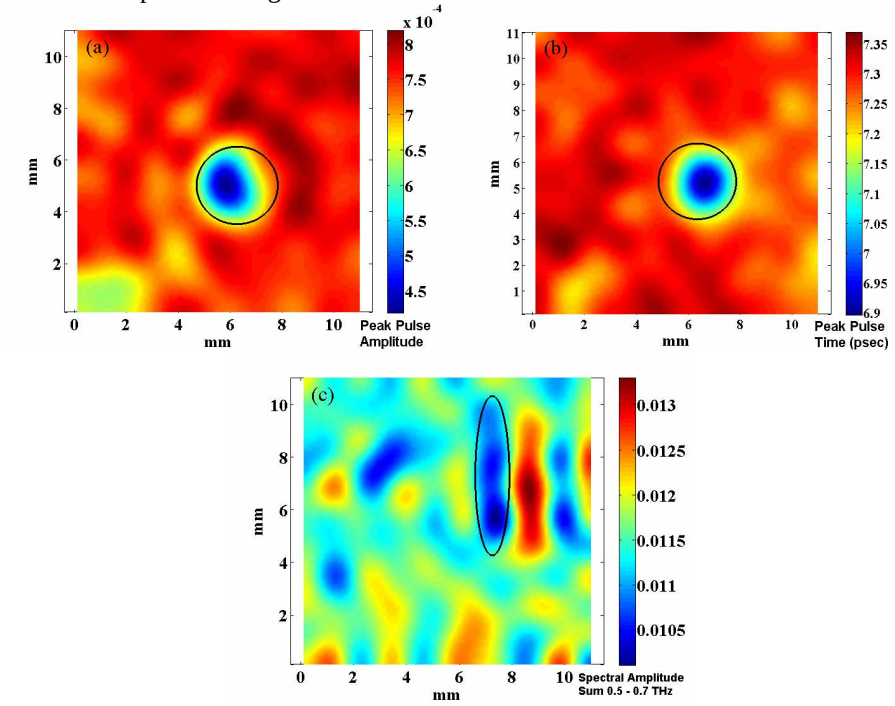

Fig. 10. THz TDS images showing 3 mm diameter milled area hidden between two glass fiber strips using (a) peak pulse amplitude and (b) peak pulse position. Linear slit void (6 mm length) (c) also hidden between two strips of glass fiber.

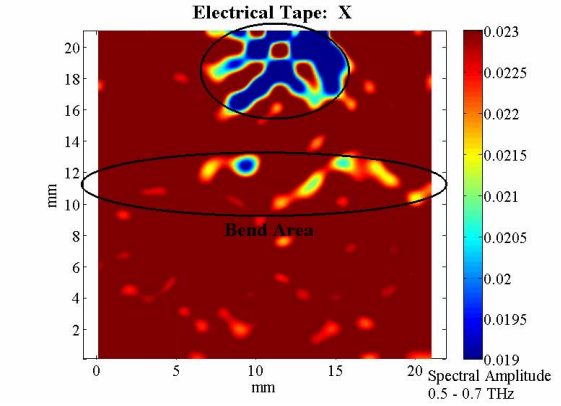

Fig. 11. THz TDS image showing bend damage across the central bend axis.

#99960 - $15.00 USD Received 11 Aug 2008; revised 6 Oct 2008; accepted 6 Oct 2008; published 10 Oct 2008

3.4 Depth of discontinuity measurement and analysis

The previous experiments demonstrated the imaging of voids in a two-dimensional plane. An attempt was made to use THz TDS to isolate a void in the third dimension of depth using the time domain. The goal was to use THz TDS to find Fabry-Perot reflections in a delaminated area of the laminated sample (#5 in Fig. 2) where the epoxy had not adhered the two glass fiber strips. The THz scans are shown in Fig. 12(a), showing the THz pulse after it had transmitted through the adhered area and the delaminated area. The autocorrelation was taken for each of the two pulses independently of each other in the attempt to show the Fabry-Perot reflections (b). Then the sample was flipped over and the process was repeated in the opposite direction (c), (d). The timing of the Fabry-Perot reflections was calculated with $T_{FP-ref} = 2n_{gf}l$ where n_{gf} is the index of the glass fiber and l is the thickness of a delaminated piece. Given that the index of refraction is 2.05 and that the thickness of the two layers is approximately 0.23 mm and 0.92 mm, the predicted times would be 3.12 psec and 12.5 psec. The first Fabry-Perot reflection occurred at approximately 3.3 psec after the main pulse in the autocorrelations. The approximate location of the second Fabry-Perot reflection is shown; however, the autocorrelation is difficult to identify on the graph. The Fabry-Perot reflections show up similarly in both directions, indicating the ambiguity in determination of depth using a transmissive setup.

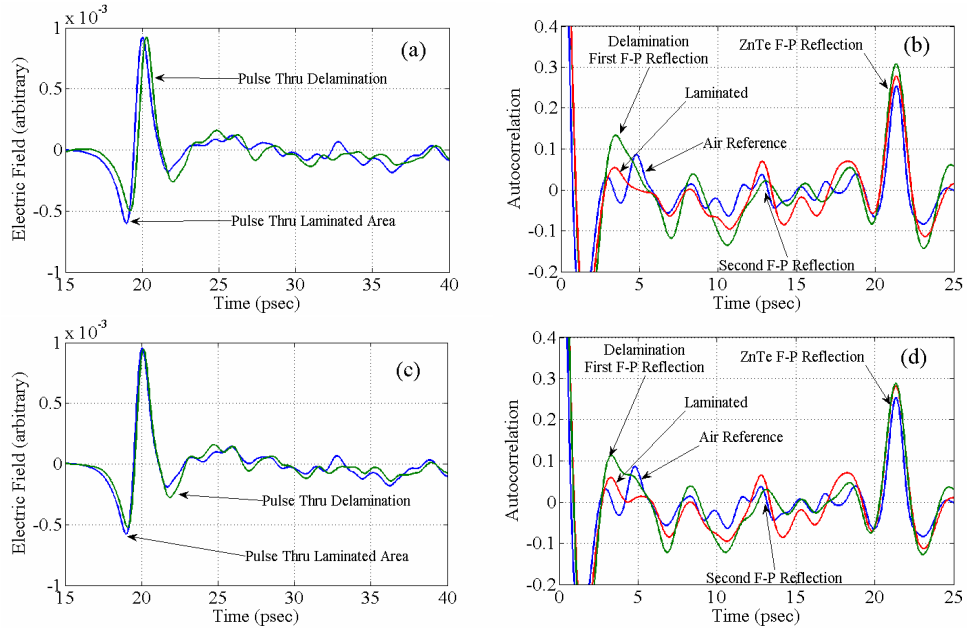

Fig. 12. THz pulses after propagating through (a) laminated and delaminated portions of a glass fiber strip. (b) Autocorrelation of each of the two pulses showing the approximate location of Fabry-Perot reflections. THz pulse propagation in the opposite direction showing pulses and their autocorrelations (c), (d).

The attenuation of the THz signal can be estimated based on the measured absorption coefficient of the glass fiber ($T_{FP}(\omega) = R(\omega)\exp(-\alpha(\omega)l)$) where $R(\omega)$ is the reflection of the signal off of the two air-sample interfaces. The amount of terahertz radiation, relative to the initial pulse, that is transmitted through the glass fiber composite after undergoing a single Fabry-Perot reflection is shown in Fig. 13. One can observe in the figure that unless a delamination is very thin (~ 0.23 mm) the reflection is unlikely to be recognizable above the system response.

#99960 - $15.00 USD Received 11 Aug 2008; revised 6 Oct 2008; accepted 6 Oct 2008; published 10 Oct 2008

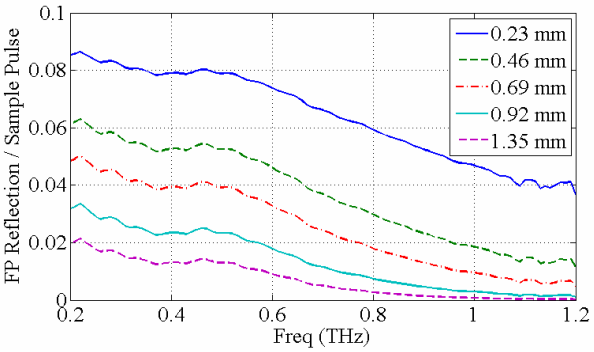

Fig. 13. Chart showing the relative strength of the first Fabry-Perot reflection after traveling through various thicknesses of glass fiber material.

5. Conclusions

THz TDS has several potential advantages over other nondestructive evaluation methods for inspection of aircraft glass fiber composites. Both ultrasound and eddy current techniques require that the source and detector remain in contact with the aircraft. In addition, eddy current testing requires that the material is conductive, which is not applicable to glass fiber. X-ray techniques use ionizing radiation to penetrate the sample which can cause safety issues for operators. X-rays can also require the use of penetrates to help detect delaminations. Video inspection can be time consuming and prone to human error. THz can penetrate glass fiber without contacting it, with submillimeter resolution, and can detect surface defects, hidden voids, delaminations, and bending damage in composites. Additionally, it can also be used to evaluate whether the aircraft composite has been chemically altered from engine burn damage by measurement of its index of refraction and absorption coefficient spectrum.

Effective medium approximations were used to estimate the refractive index of the glass weave after measuring the polyimide and glass fiber composite separately. These indices of refraction were then used to calculate the scattering properties of the composite and estimates of the scattering coefficient were low for the THz spectrum due to the similarity of the indices of refraction for the two composite materials. An aircraft glass fiber composite with various forms of damage was examined using a transmissive THz TDS system. Indices of refraction and absorption coefficients in the terahertz frequency range were measured using THz TDS in transmission configuration for comparison of damaged and undamaged material states. Results showed that localized heat damage did not noticeably change the material properties of the composite sample, however, changes in the terahertz signal were observed due to material blistering and/or residue deposited. The approximate depth of a delamination could be determined in the time domain by measuring the timing of a Fabry-Perot reflection through a thin slice of the composite. A hidden circular void was imaged and there was also evidence that areas of damage from mechanical bending stress and simulated hidden cracks could be detected with terahertz TDS imaging.

THz TDS in transmission setup was effective in locating voids at any depth or thickness, but had difficulty in finding damage that was smaller than THz wavelengths. Burn spots could be detected and the dielectric properties of polyimide appeared to remain unaltered at burn temperatures below 480°C. Additional burn tests at temperatures approaching 480°C would have to be attempted to see if and when the material properties of the composite would change. A THz TDS system in reflection mode would be a more likely candidate for inspection of glass fiber composites on aircraft and would likely be more effective in determining the depth of damage areas. The glass fiber composite absorbs a significant amount of the THz radiation, attenuating the signal, and limiting the use of Fabry-Perot

#99960 - $15.00 USD Received 11 Aug 2008; revised 6 Oct 2008; accepted 6 Oct 2008; published 10 Oct 2008

reflections for depth measurements. In reflection mode, the magnitude of the first surface reflection and subsequent reflections would be approximately the same, which should enable a greater ability to locate the depth of a void. These reflection measurements are in progress and will be reported in the near future.

Acknowledgments

The glass fiber composite samples used in this research were provided by the Air Force Research Laboratory Materials and Manufacturing Directorate, Wright Patterson AFB, OH. This research effort was partially funded by the Air Force Office of Scientific Research.

#99960 - $15.00 USD Received 11 Aug 2008; revised 6 Oct 2008; accepted 6 Oct 2008; published 10 Oct 2008